PHYSICAL REVIEW B VOLUME 37, NUMBER 16 1 JUNE 1988

Surface spin waves of semi-infinite two-sublattice ferrimagnets

Hang Zheng
Center of Theoretical Physics, Chinese Center of Advanced Science and Technology (World Laboratory), Beijing, People's Republic of China
and Department of Applied Physics, Shanghai Jiao Tong University, Shanghai, People's Republic of China

D. L. Lin
Department of Physics and Astronomy, State University of New York at Buffalo, Amherst, New York 14260
(Received 24 August 1987)

We investigate the surface spin waves on the (001) free surface of semi-infinite two-lattice ferrimagnets on the Heisenberg model with nearest-neighbor exchange interactions. Energy spectra are calculated for both NaCl and CsCl structures by means of the method of the retarded-Green's-function equation of motion. It is found that the surface-spin-wave spectrum for NaCl structure has both optical and acoustic branches, while it can only have one of these branches in the case of CsCl structure. The nature of the energy spectrum branch depends upon which sublattice the surface layer belongs to. It is also found in CsCl structure that the surface optical branch crosses into the bulk acoustic continuum and produces the resonant state. Possible extension of the theory to interface and superlattice problems is discussed.

I. INTRODUCTION

Surface spin waves (SSW's) of ferromagnets or antiferromagnets have been the subject of extensive study.[1–10] Most of the discussions have been concerned with one of two types of geometry, a semi-infinite or a slab Heisenberg ferromagnet.

Mills and Maradudin[1] first discussed the existence of surface states near the (001) surface of a Heisenberg ferromagnet with a simple cubic (sc) lattice. They also studied the effects of the surface state on thermodynamical properties of the magnet. The first investigation of the surface state in antiferromagnets was performed by Mills and Saslow[3] who studied the (001) free surface of a two-sublattice Heisenberg antiferromagnet with a body-centered-cubic (bcc) lattice. DeWames and Wolfram[4] investigated in their series of papers the effect of surface perturbations on surface modes in ferromagnets, bcc antiferromagnets, and sc antiferromagnets. The next-nearest-neighbor exchange interaction was considered by Harada and Nagai[5] in their discussions of the surface modes of semi-infinite and slab Heisenberg ferromagnets and antiferromagnets.

The method of retarded Green's function was introduced by Diep-The-Hung *et al.*[6] in their study of spin waves and other magnetic properties of ferromagnetic and antiferromagnetic films. It has also been applied by Selzer and Majlis[7] to study the surface spin waves, surface magnetization, and surface Curie temperature of a semi-infinite Heisenberg ferromagnet. The treatment of such surface magnetic problems has recently been generalized to the interface of two different Heisenberg ferromagnets by Yaniv[8] and by Bu Xing Xu *et al.*[9] More recently, Dobrzynski *et al.*[10] investigated the properties of SSW's in a superlattice.

As we have mentioned above, most of the SSW works are concerned with ferromagnets. Few are for antiferromagnets, and to our knowledge, there does not exist any work on ferrimagnets. Since the magnetization vectors of individual sublattices do not offset each other in ferrimagnets, they are more complicated than ferromagnets or antiferromagnets to handle. The spin waves and magnetic properties of bulk ferrimagnets have been investigated by the present authors[11] on the two-sublattice Heisenberg model. This paper will be referred to as I from now on. The method introduced in I is now employed to study surface spin waves near the (001) free surface of semi-infinite two-sublattice ferrimagnets.

As in I, we consider two different kinds of magnetic ions a and b. They may form either NaCl or CsCl structure with mean values of a-sublattice spin $\langle S^z\rangle_a$ and b-sublattice spin $\langle S^z\rangle_b$, respectively. For ferrimagnets, we have $|\langle S^z\rangle_a| \neq |\langle S^z\rangle_b|$ in general. In the case of ferromagnets or antiferromagnets, the energy spectrum of either bulk or surface spin waves, when expressed in terms of the dimensionless quantity $\varepsilon = E/zJ\langle S^z\rangle$, is independent of $\langle S^z\rangle$. This is no longer true in the case of ferrimagnets. The spin wave depends on the ratio $-\langle S^z\rangle_b/\langle S^z\rangle_a = \alpha$ even when expressed in unit of the same dimensionless quantity ε. For definiteness, we assume as in I, $\alpha \leq 1$ without loss of generality. Namely, the a sublattice is assumed to have a larger mean spin than the b sublattice.

This paper is organized as follows. We first review very briefly the method of retarded Green's function and obtain the matrix equation of motion for the two-sublattice bulk system in Sec. II. The method is then applied to NaCl structure in Sec. III in which we describe the cleavage procedures to create a semi-infinite ferrimagnet with (001) free surface. The resulting supermatrix equation is solved in the approximation in which the mean spin in any lattice plane of the sublattice is assumed to be independent of its distance from the surface. That is, $\langle S_{\mathrm{a}}^z\rangle=\langle S^z\rangle_a$ and $\langle S_{\mathrm{b}}^z\rangle=\langle S^z\rangle_b$. The SSW spectra are explicitly calculated and it is shown that for the special case, $\alpha=1$, our results agree completely with those for antiferromagnets. The CsCl-structure ferrimagnet is considered in Sec. IV. It is noted that parallel to the (001) surface, the crystal consists of alternative layers of a spins and b spins with equal distances and hence, can be regarded as the simplest superlattice. We find that the SSW spectrum for this structure depends upon the nature of the surface layer which may either be the a spin or the b spin. Our conclusions are discussed in Sec. V.

II. THEORY

For a bulk two-sublattice ferrimagnet, the retarded-Green's-function equations of motion have been derived and solved in I. Here we only summarize what are essential to our discussions in the following.

In either NaCl or CsCl structure, the nearest neighbors of an a spin in the a lattice are all b spins and vice versa. We use Heisenberg model Hamiltonian with nearest-neighbor interactions,

$$H=\sum_{\langle \mathrm{a},\mathrm{b}\rangle} J\mathbf{S}_{\mathrm{a}}\cdot\mathbf{S}_{\mathrm{b}}\ , \tag{1}$$

where J stands for the nearest-neighbor exchange integral, and the sum is taken over every nearest-neighboring pair only once. The method of retarded Green's function has been discussed in great detail by many authors.[12-15] The equations of motion for the spin operators $\mathbf{S}_{\mathrm{a}}$ and $\mathbf{S}_{\mathrm{b}}$ in different sublattices are obtained after the random-phase-approximation decoupling. The Fourier transform of the retarded Green's functions are then shown to satisfy a set of coupled equations that can be written as a matrix equation

$$(E\underline{1}-\underline{D})\underline{g}(\boldsymbol{\kappa},E;m,n)-\underline{F}[\underline{g}(\boldsymbol{\kappa},E;m+1,n)+\underline{g}(\boldsymbol{\kappa},E;m-1,n)]=\delta_{m,n}\underline{1}\ , \tag{2a}$$

for the NaCl structure, and

$$(E\underline{1}-\underline{D}')\underline{g}(\boldsymbol{\kappa},E;m,n)-\underline{F}_1\underline{g}(\boldsymbol{\kappa},E;m+1,n)-\underline{F}_2\underline{g}(\boldsymbol{\kappa},E;m-1,n)=\delta_{m,n}\underline{1}\ , \tag{2b}$$

for the CsCl structure. In these equations we have defined the unit matrix $\underline{1}$, and

$$\underline{g}(\boldsymbol{\kappa},E;m,n)=\begin{bmatrix} g_{aa}(\boldsymbol{\kappa},E;m,n) & g_{ab}(\boldsymbol{\kappa},E;m,n)\\ g_{ba}(\boldsymbol{\kappa},E;m,n) & g_{bb}(\boldsymbol{\kappa},E;m,n)\end{bmatrix}, \tag{3a}$$

for NaCl structure and

$$\underline{g}(\boldsymbol{\kappa},E;m,n)=\begin{bmatrix} g_{aa}(\boldsymbol{\kappa},E;m,n) & g_{ab}(\boldsymbol{\kappa},E;m,n-\frac{1}{2})\\ g_{ba}(\boldsymbol{\kappa},E;m-\frac{1}{2},n) & g_{bb}(\boldsymbol{\kappa},E;m-\frac{1}{2},n-\frac{1}{2})\end{bmatrix}, \tag{3b}$$

for CsCl structure where $g_{aa}(\boldsymbol{\kappa},E;m,n)$ is the Fourier transform of the retarded Green's function and is expressed in the Bloch-Wannier representation. That is, the motion in the xy plane is described by Bloch function and in the z direction by Wannier function. The matrices $\underline{D}$ and $\underline{F}$ in (2) are defined by

$$\underline{D}=\begin{bmatrix} -6J\langle S^z\rangle_b & 4J\langle S^z\rangle_a\xi(\boldsymbol{\kappa})\\ 4J\langle S^z\rangle_b\xi(\boldsymbol{\kappa}) & -6J\langle S^z\rangle_a\end{bmatrix}, \tag{4a}$$

$$\underline{F}=\begin{bmatrix} 0 & J\langle S^z\rangle_a\\ J\langle S^z\rangle_b & 0\end{bmatrix}, \tag{4b}$$

for NaCl structure and

$$\underline{D}'=\begin{bmatrix} -8J\langle S^z\rangle_b & 4J\langle S^z\rangle_a\eta(\boldsymbol{\kappa})\\ 4J\langle S^z\rangle_b\eta(\boldsymbol{\kappa}) & -8J\langle S^z\rangle_a\end{bmatrix}, \tag{5a}$$

$$\underline{F}_1=\begin{bmatrix} 0 & 4J\langle S^z\rangle_a\eta(\boldsymbol{\kappa})\\ 0 & 0\end{bmatrix}, \tag{5b}$$

$$\underline{F}_2=\begin{bmatrix} 0 & 0\\ 4J\langle S^z\rangle_b\eta(\boldsymbol{\kappa}) & 0\end{bmatrix}, \tag{5c}$$

for CsCl structure. The two-dimensional wave vector $\boldsymbol{\kappa}$ is defined by the three-dimensional vector $\mathbf{k}=(\boldsymbol{\kappa},q)=(k_x,k_y,q)$. The ion layers in a and b sublattice are labeled differently. In the case of NaCl structure, both sublattice layers are labeled by the integers $0,\pm1,\pm2,\ldots$; and in the case of CsCl, a-sublattice layers are denoted by integers and b-sublattice layers by half-integers $\pm\frac{1}{2},\pm\frac{3}{2},\ldots$. The functions ξ and η are given by

$$\xi(\boldsymbol{\kappa})=\tfrac{1}{2}[\cos(k_xd)+\cos(k_yd)]\ , \tag{6a}$$

$$\eta(\boldsymbol{\kappa})=\cos(k_xd)\cos(k_yd)\ , \tag{6b}$$

where d represents the nearest neighbor distance. Combining equations of the type of (2b) for all layers m, we obtain the supermatrix equation for CsCl structure

$$\begin{bmatrix} & \vdots & & & & \\ \cdots\ E\underline{1}-\underline{D}' & -\underline{F}_2 & 0 & & & \\ -\underline{F}_1 & E\underline{1}-\underline{D}' & -\underline{F}_2 & 0 & & \\ 0 & -\underline{F}_1 & E\underline{1}-\underline{D}' & -\underline{F}_2 & 0 & \\ & 0 & -\underline{F}_1 & E\underline{1}-\underline{D}' & -\underline{F}_2 & \\ & & 0 & -\underline{F}_1 & E\underline{1}-\underline{D}' & \cdots \\ & & & & \vdots & \end{bmatrix}\begin{bmatrix}\vdots\\ \underline{g}(\boldsymbol{\kappa},E;2,n)\\ \underline{g}(\boldsymbol{\kappa},E;1,n)\\ \underline{g}(\boldsymbol{\kappa},E;0,n)\\ \underline{g}(\boldsymbol{\kappa},E;-1,n)\\ \underline{g}(\boldsymbol{\kappa},E;-2,n)\\ \vdots\end{bmatrix}=\begin{bmatrix}\vdots\\ \delta_{2,n}\underline{1}\\ \delta_{1,n}\underline{1}\\ \delta_{0,n}\underline{1}\\ \delta_{-1,n}\underline{1}\\ \delta_{-2,n}\underline{1}\\ \vdots\end{bmatrix} \tag{7}$$

in which every matrix element is a 2×2 matrix. A similar supermatrix equation for NaCl structure follows if one makes the replacements in (7) $\underline{D}'=\underline{D}$ and $\underline{F}_1=\underline{F}_2=\underline{F}$.

We are now ready to consider semi-infinite ferrimagnets with (001) free surface which is created by the cleavage procedure.[16] The NaCl and CsCl structure will be treated separately in the following sections.

III. SURFACE SPIN WAVES IN NaCl STRUCTURE

After the cleavage plane passes through the crystal between the ion layers of $m=-1$ and 0, the bulk crystal is cleaved into two semi-infinite ones. With all connections between them being cut off, the two matrix elements of the supermatrix connecting $m=-1$ and 0 layers should vanish. The diagonal matrix elements corresponding to these two layers should also be modified to reflect the fact that there are only five nearest neighbors to each spin instead of six. If we denote the new 2×2 matrix Green's function by

$$\underline{G}(\boldsymbol{\kappa},E;m,n)=\begin{bmatrix} G_{aa}(\boldsymbol{\kappa},E;m,n) & G_{ab}(\boldsymbol{\kappa},E;m,n) \\ G_{ba}(\boldsymbol{\kappa},E;m,n) & G_{bb}(\boldsymbol{\kappa},E;m,n)\end{bmatrix}, \tag{8}$$

we find the supermatrix equation that $\underline{G}$ satisfies is

$$\begin{bmatrix} & \vdots & & & & \\ \cdots & E\underline{1}-\underline{D} & -\underline{F} & 0 & & \\ & -\underline{F} & E\underline{1}-\underline{D}-\underline{V}_s & -\underline{F}-\underline{V}_f & 0 & \\ & 0 & \underline{F}-\underline{V}_f & E\underline{1}-\underline{D}-\underline{V} & -\underline{F} & \\ & & 0 & -\underline{F} & E\underline{1}-\underline{D} & \cdots \\ & & & & \vdots & \end{bmatrix}\begin{bmatrix}\vdots \\ \underline{G}(\boldsymbol{\kappa},E;1,n) \\ \underline{G}(\boldsymbol{\kappa},E;0,n) \\ \underline{G}(\boldsymbol{\kappa},E;-1,n) \\ \vdots\end{bmatrix}=\begin{bmatrix}\vdots \\ \delta_{1,n}\underline{1} \\ \delta_{0,n}\underline{1} \\ \delta_{-1,n}\underline{1} \\ \vdots\end{bmatrix}, \tag{9}$$

where the 2×2 matrices $\underline{V}_s$ and $\underline{V}_f$ are given by

$$\underline{V}_s=\begin{bmatrix} J\langle S^z\rangle_b & 0 \\ 0 & J\langle S^z\rangle_a\end{bmatrix}, \tag{10a}$$

$$\underline{V}_f=\begin{bmatrix} 0 & -J\langle S^z\rangle_a \\ -J\langle S^z\rangle_b & 0\end{bmatrix}. \tag{10b}$$

To simplify the expressions, we rewrite the coefficient matrix in (7) in terms of the supermatrices $\underline{E}$ and $\underline{H}_0$ as $\underline{E}-\underline{H}_0$. Then (7) becomes

$$\sum_l (E-H_0)_{ml}\underline{g}(\boldsymbol{\kappa},E;l,n)=\delta_{m,n}\underline{1}\ , \qquad m=\ldots,-1,0,1,\ldots, \tag{11}$$

where the matrix element $(E-H_0)_{ml}$ itself is a 2×2 matrix. Similarly, Eq. (9) becomes

$$\sum_l (E-H_0-V)_{ml}\underline{G}(\boldsymbol{\kappa},E;l,n)=\delta_{m,n}\underline{1}\ , \qquad m=\ldots,-1,0,1,\ldots, \tag{12}$$

where the supermatrix $\underline{V}$ has only four nonzero elements which are themselves 2×2 matrices, namely,

$$\underline{V}_{0,0}=\underline{V}_{-1,1}=\underline{V}_s\ , \tag{13a}$$

$$\underline{V}_{0,-1}=\underline{V}_{-1,0}=\underline{V}_f\ . \tag{13b}$$

It is clear that (11) has the solution

$$\underline{g}(\boldsymbol{\kappa},E;m,n)=[(E-H_0)^{-1}]_{mn}\ . \tag{14}$$

Using this form of $\underline{g}(\boldsymbol{\kappa},E;l,m)$ one can easily show that $\underline{G}(\boldsymbol{\kappa},E;m,n)$ satisfies the Dyson equation

$$\underline{G}(\boldsymbol{\kappa},E;m,n)=\underline{g}(\boldsymbol{\kappa},E;m,n)+\sum_{l,l'}\underline{g}(\boldsymbol{\kappa},E;m,l)V_{ll'}\underline{G}(\boldsymbol{\kappa},E;l',n)\ , \tag{15}$$

which is soluble because we know the explicit form of $\underline{g}$ from I. It should be emphasized, however, that an important assumption is already implied in the above discussion. We have assumed that the mean spin values $\langle S_{\rm a}^z\rangle$ and $\langle S_{\rm b}^z\rangle$ remain to be constant everywhere. This is, of course, not the case because the surface has destroyed the translational symmetry in the z direction. Hence, the mean-spin values of either sublattice should depend upon the distance from the surface. If this z dependence was taken into account, the supermatrix V would have infinite number of nonzero matrix elements and it would not be possible to solve (15) anymore. Therefore, we assume, as most of the other authors do in their treatment of surface problems,[1–5,8,9] that $\langle S_{\rm a}^z\rangle=\langle S^z\rangle_a$ and $\langle S_{\rm b}^z\rangle=\langle S^z\rangle_b$.

To solve Eq. (15), we consider the half space $m\geq 0$. Thus, for all $n\leq -1$, we have $\underline{G}(\boldsymbol{\kappa},E;m,n)=0$. The $m\leq -1$ half space can be treated in similar fashion. Using the nonzero matrix elements given by (13), we obtain from (15)

$$\underline{G}(\boldsymbol{\kappa},E;m,n)=\underline{g}(\boldsymbol{\kappa},E;m,n)+\underline{g}(\boldsymbol{\kappa},E;m,0)\underline{V}_s\underline{G}(\boldsymbol{\kappa},E;0,n)+\underline{g}(\boldsymbol{\kappa},E;m,-1)\underline{V}_f\underline{G}(\boldsymbol{\kappa},E;0,n)\ . \tag{16}$$

Equation (16) yields, when $m=0$,

$$\underline{G}(\boldsymbol{\kappa};E,0,n)=[1-\underline{g}(\boldsymbol{\kappa},E;0,0)\underline{V}_s-\underline{g}(\boldsymbol{\kappa},E;0,-1)\underline{V}_f]^{-1}\underline{g}(\boldsymbol{\kappa},E;0,n)\ . \tag{17}$$

Combining (16) and (17) we find directly

$$\underline{G}(\boldsymbol{\kappa},E;m,n)=\underline{g}(\boldsymbol{\kappa},E;m,n)+[\underline{g}(\boldsymbol{\kappa},E;m,0)\underline{V}_s+\underline{g}(\boldsymbol{\kappa},E;m,-1)\underline{V}_f]\times[1-\underline{g}(\boldsymbol{\kappa},E;0,0)\underline{V}_s-\underline{g}(\boldsymbol{\kappa},E;0,-1)\underline{V}_f]^{-1}\underline{g}(\boldsymbol{\kappa},E;0,n)\ . \tag{18}$$

This is the Green's function solution for a semi-infinite ferrimagnet with NaCl structure. The first term on the right-hand side of (18) is the bulk solution, and surface effects are involved in the second term. The pole of the 2×2 inverse matrix determines the SSW energy spectrum which is found by solving the determinant equation

$$\det|\underline{1}-\underline{g}(\boldsymbol{\kappa},E;0,0)\underline{V}_s-\underline{g}(\boldsymbol{\kappa},E;0,-1)\underline{V}_f|=0\ . \tag{19}$$

The explicit form of $\underline{g}(\boldsymbol{\kappa},E;m,n)$ has been worked out in I and is given by

$$\underline{g}(\boldsymbol{\kappa},E;m,n)=\frac{1}{N_z}\sum_q\frac{e^{iqd(m-n)}}{[(E-E_+(\boldsymbol{\kappa},q)][E-E_-(\boldsymbol{\kappa},q)]}\begin{bmatrix}E+6J\langle S^z\rangle_a & 6J\langle S^z\rangle_a\gamma_1(\mathbf{k})\\ -6\alpha J\langle S^z\rangle_a\gamma_1(\mathbf{k}) & E-6\alpha J\langle S^z\rangle_a\end{bmatrix}, \tag{20}$$

where

$$E_\pm(\mathbf{k})=-3J\langle S^z\rangle_a(1-\alpha)\pm3J\langle S^z\rangle_a[(1+\alpha)^2-4\alpha\gamma_1^2(\mathbf{k})]^{1/2}\ , \tag{21}$$

$$\gamma_1(\mathbf{k})=\tfrac{1}{3}[\cos(k_xd)+\cos(k_yd)+\cos(qd)]\ , \tag{22}$$

and the lattice spacing constant d is the period along z direction. Substituting (21) and (22) in (20) and introducing the dimensionless variable $\varepsilon=E/6J\langle S^2\rangle_a$, we find

$$\underline{g}(\boldsymbol{\kappa},E;m,n)=\frac{1}{6J\langle S^2\rangle_a}\frac{d}{2\pi}\int_{-\pi/d}^{\pi/d}\frac{dq\,e^{iqd(m-n)}}{\varepsilon^2+(1-\alpha)\varepsilon-\alpha+\alpha[\frac{2}{3}\xi(\boldsymbol{\kappa})+\frac{1}{3}\cos(qd)]^2}\begin{bmatrix}\varepsilon+1 & \frac{2}{3}\xi+\cos(qd)\\ -\alpha[\frac{2}{3}\xi+\cos(qd)] & \varepsilon-\alpha\end{bmatrix}, \tag{23}$$

where we have made the replacement

$$\frac{1}{N_z}\sum_q\to\frac{d}{2\pi}\int_{-\pi/d}^{\pi/d}dq\ .$$

The integration in (23) must be carried out for each matrix element separately. Because the denominator involves $\cos^2(qd)$, the method of integration is more complicated than but similar to that described in Ref. 16. The procedures are outlined in the Appendix and the results are

$$\underline{g}(\boldsymbol{\kappa},E;m,n)=\frac{1}{6J\langle S^2\rangle_a}\frac{3}{2}\begin{bmatrix}\frac{1+\varepsilon}{\alpha(\alpha-\varepsilon)}Z_-(\boldsymbol{\kappa}) & \frac{1}{\alpha}Z_+(\boldsymbol{\kappa})\\ -Z_+(\boldsymbol{\kappa}) & \frac{\alpha-\varepsilon}{\alpha(1+\varepsilon)}Z_-(\boldsymbol{\kappa})\end{bmatrix}, \tag{24}$$

where

$$Z_\pm(\boldsymbol{\kappa})=i\{[W_-(\boldsymbol{\kappa})]^{|m-n|}/U_-(\boldsymbol{\kappa})\pm[W_+(\boldsymbol{\kappa})]^{|m-n|}/U_+(\boldsymbol{\kappa})\}\ , \tag{25}$$

$$U_\pm(\boldsymbol{\kappa})=\begin{cases}i\,\mathrm{sgn}(T_\pm)[T_\pm^2(\boldsymbol{\kappa})-1]^{1/2}, & T_\pm^2(\boldsymbol{\kappa})>1\\ \pm\,\mathrm{sgn}\left[\varepsilon-\frac{\alpha-1}{2}\right][1-T_\pm^2(\boldsymbol{\kappa})]^{1/2}, & T_\pm^2(\boldsymbol{\kappa})<1\end{cases} \tag{26}$$

$$T_\pm(\boldsymbol{\kappa})=2\xi(\boldsymbol{\kappa})\pm3\sqrt{(1+\varepsilon)(\alpha-\varepsilon)/\alpha}\ , \tag{27}$$

$$W_\pm(\boldsymbol{\kappa})=-[T_\pm(\boldsymbol{\kappa})+iU_\pm(\boldsymbol{\kappa})]\ . \tag{28}$$

The function $\mathrm{sgn}(x)$ is defined to be $+1$ when $x>0$ and -1 when $x<0$. With the $\underline{g}$ given by (24) and the $\underline{V}$'s by (10), Eq. (19) becomes after a long calculation

$$\det\begin{vmatrix}1+\alpha J\langle S^z\rangle_a[g_{aa}(0,0)-g_{ab}(0,-1)] & -J\langle S^z\rangle_a[g_{ab}(0,0)-g_{aa}(0,-1)]\\ \alpha J\langle S^z\rangle_a[g_{ba}(0,0)-g_{bb}(0,-1)] & 1-J\langle S^z\rangle_a[g_{bb}(0,0)-g_{ba}(0,-1)]\end{vmatrix}=\frac{1}{2U_+U_-}\frac{1}{W_+W_--1}\left[5+\frac{3(\alpha-1)}{\alpha}\varepsilon+T_+T_--U_+U_-\right]=0\ , \tag{29}$$

where we have used the relation

$$W_+W_-+\frac{1}{W_+W_-}=2T_+T_--2U_+U_-\ .$$

From (27), we see that T_+T_- does not involve a square root but U_+U_- still does. To avoid the square root, we multiply (29) by the expression

$$5+\frac{3(\alpha-1)}{\alpha}\varepsilon+T_+T_-+U_+U_- . \tag{29'}$$

But since

$$\left[5+\frac{3(\alpha-1)}{\alpha}\varepsilon+T_+T_-\right]^2-(U_+U_-)^2=\frac{54}{\alpha^2}(\alpha-1)\left[\varepsilon^3+\left[\frac{5}{6}(1-\alpha)-\frac{4}{3}\frac{\alpha}{1-\alpha}\right]\varepsilon^2+\frac{4\alpha}{9}(\xi^2-4)\varepsilon+\frac{8}{9}\frac{\alpha^2}{1-\alpha}(1-\xi^2)\right] ,$$

we see immediately that as long as $\alpha\neq 1$, the SSW spectrum is determined by

$$\varepsilon^3+\left[\frac{5}{6}(1-\alpha)-\frac{4}{3}\frac{\alpha}{1-\alpha}\right]\varepsilon^2+\frac{4\alpha}{9}(\xi^2-4)\varepsilon+\frac{8}{9}\frac{\alpha^2}{1-\alpha}(1-\xi^2)=0 , \tag{30}$$

and when $\alpha=1$, it is given by

$$\varepsilon^2-\tfrac{2}{3}(1-\xi^2)=0 . \tag{31}$$

It must be pointed out, however, that the three roots obtained from (30) must be checked because an extra expression has been multiplied. We must make sure that the root does not make the expression (29′) vanish. As a matter of fact, only two of the three roots satisfy these requirements and therefore represent the true SSW spectra.

Equation (30) can be solved in a standard way[17] and the three roots are

$$\varepsilon_1(\boldsymbol{\kappa})=[-\tfrac{4}{3}P(\boldsymbol{\kappa})]^{1/2}\cos\theta(\boldsymbol{\kappa})-\frac{1}{3}\left[\frac{5}{6}(1-\alpha)-\frac{4}{3}\frac{\alpha}{1-\alpha}\right] , \tag{32a}$$

$$\varepsilon_2(\boldsymbol{\kappa})=[-\tfrac{4}{3}P(\boldsymbol{\kappa})]^{1/2}\cos\left[\theta(\boldsymbol{\kappa})+\frac{2\pi}{3}\right]-\frac{1}{3}\left[\frac{5}{6}(1-\alpha)-\frac{4}{3}\frac{\alpha}{1-\alpha}\right] , \tag{32b}$$

$$\varepsilon_3(\boldsymbol{\kappa})=[-\tfrac{4}{3}P(\boldsymbol{\kappa})]^{1/2}\cos\left[\theta(\boldsymbol{\kappa})+\frac{4\pi}{3}\right]-\frac{1}{3}\left[\frac{5}{6}(1-\alpha)-\frac{4}{3}\frac{\alpha}{1-\alpha}\right] , \tag{32c}$$

$$P(\boldsymbol{\kappa})=\frac{4\alpha}{9}(\xi^2-4)-\frac{1}{3}\left[\frac{5}{6}(1-\alpha)-\frac{4}{3}\frac{\alpha}{1-\alpha}\right]^2 , \tag{33a}$$

$$Q(\boldsymbol{\kappa})=\frac{8}{9}\frac{\alpha^2}{1-\alpha}(1-\xi^2)-\frac{4\alpha}{27}(\xi^2-4)\times\left[\frac{5}{6}(1-\alpha)-\frac{4}{3}\frac{\alpha}{1-\alpha}\right]+\frac{2}{27}\left[\frac{5}{6}(1-\alpha)-\frac{4}{3}\frac{\alpha}{1-\alpha}\right]^3 , \tag{33b}$$

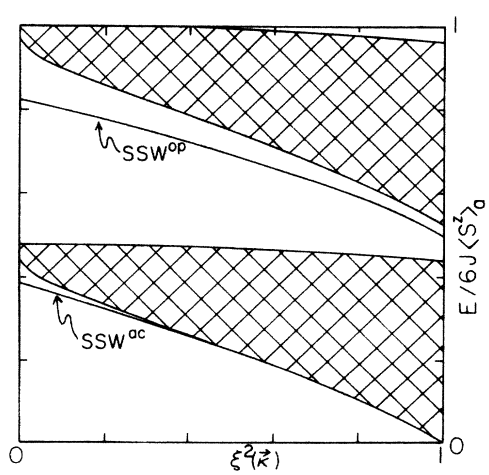

FIG. 1. Optical (op) and acoustic (ac) branches of the SSW spectrum of NaCl structure ferrimagnet, $S_a=1$, $S_b=0.5$, $\alpha=0.476$, and $\langle S^z\rangle_a=0.944$. The corresponding bulk spectrum (shaded area) is also shown for comparison.

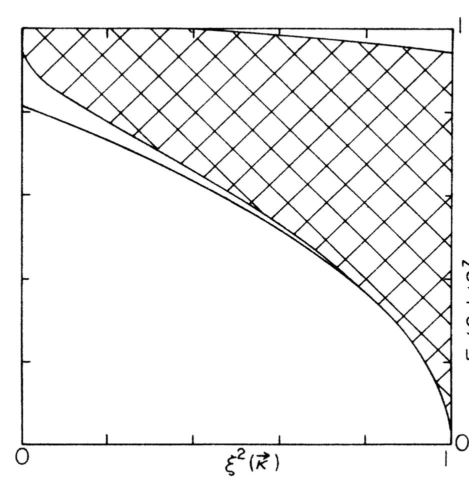

FIG. 2. SSW spectrum of NaCl structure antiferromagnet, $S_a=S_b$ and $\alpha=1$. The shaded area shows the corresponding bulk spectrum.

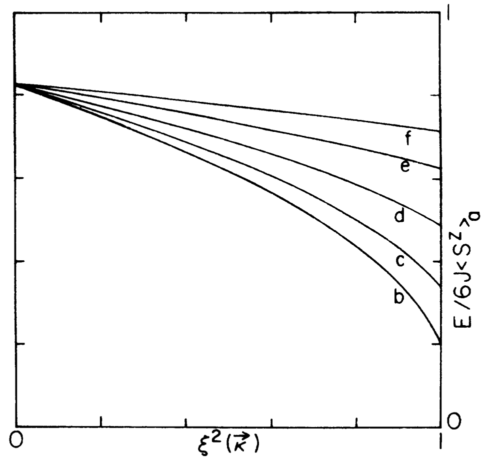

FIG. 3. Optical branch of the SSW spectrum on (001) free surface of NaCl structure ferrimagnet. b: $S_a=2.5$, $S_b=2$, $\alpha=0.794$; c: $S_a=1.5$, $S_b=1$, $\alpha=0.651$; d: $S_a=2$, $S_b=1$, $\alpha=0.486$; e: $S_a=1.5$, $S_b=0.5$, $\alpha=0.316$; f: $S_a=2.5$, $S_b=0.5$, $\alpha=0.192$.

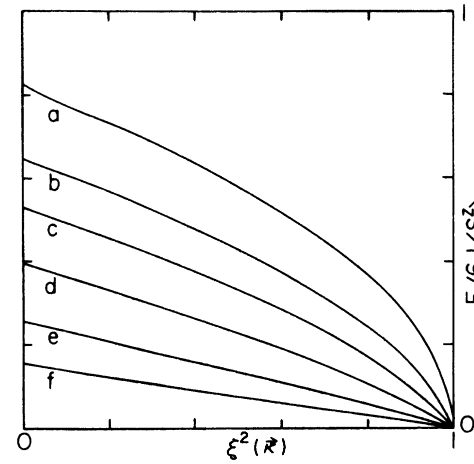

FIG. 4. Acoustic branch of the SSW spectrum on (001) free surface of NaCl structure ferrimagnet. All the parameters for the curves b–f are the same as in Fig. 3 except for a for which $S_a=S_b$ and $\alpha=1$.

$$R(\boldsymbol{\kappa})=P^3/27+Q^2/4\ , \tag{33c}$$

$$\theta(\boldsymbol{\kappa})=\frac{\pi}{6}-\tfrac{1}{3}\arctan[-Q(\boldsymbol{\kappa})/2\sqrt{-R(\boldsymbol{\kappa})}]\ . \tag{34}$$

It is noted that $R<0$ when $\alpha\le 1$ and $\xi^2\le 1$, as can be directly verified. Equation (33c) then implies that $P<0$.

By numerical computation we find that $\varepsilon_1(\boldsymbol{\kappa})$ does not satisfy the conditions discussed above while both ε_2 and ε_3 do. In fact, we find that for $0<\alpha<1$ and $\xi^2(\boldsymbol{\kappa})\le 1$, $\varepsilon_2(\boldsymbol{\kappa})<0$ and $\varepsilon_3(\boldsymbol{\kappa})\ge 0$. As has been discussed in I, the negative energy state should be occupied by the "particle" even in the ground state. Physically observed spin-wave excited state is actually the negative energy hole. Hence the SSW excited spectrum of the (001) free surface of a sc lattice ferrimagnet has two branches, optical branch $\varepsilon_{\rm SSW}^{\rm op}(\boldsymbol{\kappa})$ and acoustic branch $\varepsilon_{\rm SSW}^{\rm ac}(\boldsymbol{\kappa})$. Thus

$$\varepsilon_{\rm SSW}^{\rm op}(\boldsymbol{\kappa})=-\varepsilon_2(\boldsymbol{\kappa})\ , \tag{35a}$$

$$\varepsilon_{\rm SSW}^{\rm ac}(\boldsymbol{\kappa})=\varepsilon_3(\boldsymbol{\kappa})\ , \tag{35b}$$

because $\varepsilon_2(\boldsymbol{\kappa})\neq 0$ when $\xi^2(\boldsymbol{\kappa})=1$ and $\varepsilon_3(\boldsymbol{\kappa})=0$ when $\xi^2(\boldsymbol{\kappa})=1$.

When $\alpha=1$, the system is antiferromagnetic. The SSW spectrum in this case takes a very simple form of (31) which is identical to that of the free surface in the third paper of Ref. 4.

Our results are plotted in Figs. 1–4 for different cases. In Fig. 1 we plot SSW spectrum along with the bulk spin-wave spectrum (shaded area) for comparison. Figure 2 shows the SSW and bulk spin-wave spectra for the case of antiferromagnet. The optical branch of SSW spectrum for different α values are shown in Fig. 3 and acoustic branch of SSW for different α values are plotted in Fig. 4.

IV. SURFACE SPIN WAVES IN CsCl STRUCTURE

For the case of CsCl structure, semi-infinite ferrimagnets with (001) free surface can again be made by cleavage. Now we assume that the cleavage plane passes through the crystal between the -1 layer of a lattice and the $-\frac{1}{2}$ layer of b lattice. One of the resulting semi-infinite ferrimagnets occupies the half space with $z\ge -\frac{1}{2}a_0=-d$, and its surface layer belongs to the b sublattice. The other occupies the half space with $z\le -a_0=-2d$, and its surface layer belongs to the a sublattice. As we shall see later, the SSW spectra associated with these two surfaces are qualitatively different.

The 2×2 matrix of Green's functions after cleavage is

$$\underline{G}(\boldsymbol{\kappa},E;m,n)=\begin{bmatrix} G_{aa}(\boldsymbol{\kappa},E;m,n) & G_{ab}(\boldsymbol{\kappa},E;m,n-\frac{1}{2}) \\ G_{ba}(\boldsymbol{\kappa},E;m-\frac{1}{2},n) & G_{bb}(\boldsymbol{\kappa},E;m-\frac{1}{2},n-\frac{1}{2}) \end{bmatrix}. \tag{36}$$

The equation that $\underline{G}$ satisifes can be obtained from (7) by taking into account the effects of cleavage. As a matter of fact, only four elements of the coefficient matrix are influenced in our approximation of nearest neighbor exchange interactions. If we define the 2×2 matrices

$$\begin{gathered}\underline{V}_{ba}=\begin{bmatrix} 4J\langle S^z\rangle_b & 0 \\ 0 & 0\end{bmatrix},\quad \underline{V}_{bb}=\begin{bmatrix} 0 & 0 \\ 0 & 4J\langle S^z\rangle_a\end{bmatrix},\\ \underline{V}_{1f}=\begin{bmatrix} 0 & -4J\langle S^z\rangle_a\eta(\boldsymbol{\kappa}) \\ 0 & 0\end{bmatrix},\quad \underline{V}_{2f}=\begin{bmatrix} 0 & 0 \\ -4J\langle S^z\rangle_b\eta(\boldsymbol{\kappa}) & 0\end{bmatrix},\end{gathered} \tag{37}$$

we find the supermatrix equation that $\underline{G}$ satisfies

$$\begin{bmatrix} & \vdots & & & & \\ \cdots\ E\underline{1}-\underline{D}' & -\underline{F}_2 & 0 & & & \\ -\underline{F}_1 & E\underline{1}-\underline{D}' & -\underline{F}_2 & 0 & & \\ 0 & -\underline{F}_1 & E\underline{1}-\underline{D}'-\underline{V}_{bb} & -\underline{F}_2-\underline{V}_{2f} & 0 & \\ & 0 & -\underline{F}_1-\underline{V}_{1f} & E\underline{1}-\underline{D}'-\underline{V}_{ab} & -\underline{F}_2 & \\ & & 0 & -\underline{F}_1 & E\underline{1}-\underline{D}' & \cdots \\ & & & & \vdots & \end{bmatrix} \begin{bmatrix} \vdots \\ \underline{G}(\boldsymbol{\kappa},E;2,n) \\ \underline{G}(\boldsymbol{\kappa},E;1,n) \\ \underline{G}(\boldsymbol{\kappa},E;0,n) \\ \underline{G}(\boldsymbol{\kappa},E;-1,n) \\ \underline{G}(\boldsymbol{\kappa},E;-2,n) \\ \vdots \end{bmatrix} = \begin{bmatrix} \vdots \\ \delta_{2,n}\underline{1} \\ \delta_{1,n}\underline{1} \\ \delta_{0,n}\underline{1} \\ \delta_{-1,n}\underline{1} \\ \delta_{-2,n}\underline{1} \\ \vdots \end{bmatrix} . \tag{38}$$

From Eqs. (5) and (37), we see that the effect of $\underline{V}_{1f}$ and $\underline{V}_{2f}$ is to cut off the connection between $-\frac{1}{2}$ and -1 layers, and the effect of $\underline{V}_{bb}$ and $\underline{V}_{ba}$ is to reflect the change in coordination number from 8 to 4 for ions on the free surface.

A similar procedure as described in Sec. III then leads to the Dyson equation

$$\underline{G}(\boldsymbol{\kappa},E;m,n)=\underline{g}(\boldsymbol{\kappa},E;m,n)+\sum_{l,l'}\underline{g}(\boldsymbol{\kappa},E;m,l)V_{ll'}\underline{G}(\boldsymbol{\kappa},E;m,l',n) , \tag{39}$$

where the supermatrix $\underline{V}$ has only four nonvanishing matrix elements

$$\begin{aligned} &\underline{V}_{0,0}=\underline{V}_{bb},\quad \underline{V}_{-1,-1}=\underline{V}_{ba} ,\\ &\underline{V}_{-1,0}=\underline{V}_{1f},\quad \underline{V}_{0,-1}=\underline{V}_{2f} . \end{aligned} \tag{40}$$

We remark that the same assumption of constant mean spin values has been made here as in the case of NaCl structure.

Since the two semi-infinite systems resulted from the cleavage have their surface layers belonging to different sublattices, we treat them separately. Consider first $m\geq 0$, $n\geq 0$ or the system with surface layer of b-sublattice ions. Equation (39) can be solved by the same method as before. That is, set $m=0$ in (39) and solve for $\underline{G}(\boldsymbol{\kappa},E;0,n)$ which is then substituted back in (39) to obtain the result,

$$\begin{aligned} \underline{G}(\boldsymbol{\kappa},E;m,n)=\underline{g}(\boldsymbol{\kappa},E;m,n)+[\underline{g}(\boldsymbol{\kappa},E;m,0)\underline{V}_{bb} \\ +\underline{g}(\boldsymbol{\kappa},E;m,-1)\underline{V}_{1f}][1-\underline{g}(\boldsymbol{\kappa},E;0,0)\underline{V}_{bb}-\underline{g}(\boldsymbol{\kappa},E;0,-1)\underline{V}_{1f}]^{-1}\underline{g}(\boldsymbol{\kappa},E;0,n) . \end{aligned} \tag{41}$$

The SSW spectrum is therefore determined by

$$\det|\underline{1}-\underline{g}(\boldsymbol{\kappa},E;0,0)\underline{V}_{bb}-\underline{g}(\boldsymbol{\kappa},E;0,-1)\underline{V}_{1f}|=0 . \tag{42}$$

The explicit form of $\underline{g}(\boldsymbol{\kappa},E;m,n)$ has again been found in I. It is

$$\underline{g}(\boldsymbol{\kappa},E;m,n)=\frac{1}{N_z}\sum_q \frac{e^{2iqd(m-n)}}{[E-E_+(\mathbf{k})][E-E_-(\mathbf{k})]}\begin{bmatrix} E+8J\langle S^z\rangle_a & 8J\langle S^z\rangle_a\gamma_2(\mathbf{k})e^{iqd} \\ -8\alpha J\langle S^z\rangle_a\gamma_2(\mathbf{k})e^{-iqd} & E-8\alpha J\langle S^z\rangle_a \end{bmatrix} , \tag{43}$$

where

$$E_\pm(\mathbf{k})=-4J\langle S^z\rangle_a(1-\alpha)\pm 4J\langle S^z\rangle_a[(1+\alpha)^2-4\alpha\gamma_2^2(\mathbf{k})]^{1/2} , \tag{43a}$$

$$\gamma_2(\mathbf{k})=\cos(\kappa_x d)\cos(\kappa_y d)\cos(qd) , \tag{43b}$$

and $a_0=2d$ is the period in z direction for the CsCl structure. By introducing the dimensionless variable $\varepsilon=E/8J\langle S^z\rangle_a$ and making the replacement

$$\frac{1}{N_z}\sum_q \to \frac{2d}{2\pi}\int_{-\pi/2d}^{\pi/2d} dq ,$$

we have

$$\underline{g}(\boldsymbol{\kappa},E;m,n)=\frac{1}{8J\langle S^z\rangle_a}\frac{1}{2\pi}\int_{-\pi}^{\pi}dp\frac{e^{ip(m-n)}}{\varepsilon^2+(1-\alpha)\varepsilon-\alpha+\frac{\alpha}{2}\eta^2+\frac{\alpha}{2}\eta^2\cos p}\begin{bmatrix} \varepsilon+1 & \frac{1}{2}\eta(1+e^{ip}) \\ \frac{-\alpha}{2}\eta(1+e^{-ip}) & \varepsilon-\alpha \end{bmatrix} , \tag{44}$$

where we have defined $p=2qd$ and η stands for $\eta(\boldsymbol{\kappa})$ for simplicity. The integrals are again evaluated in the complex z plane by applying the residue theorem as outlined in the Appendix. The result is

$$\underline{g}(\boldsymbol{\kappa},E;m,n)=\frac{1}{8J\langle S^2\rangle_a}\frac{1}{\frac{\alpha}{2}\eta^2(\boldsymbol{\kappa})}\begin{bmatrix} (\varepsilon+1)\frac{1}{U(\boldsymbol{\kappa})}W^{|m-n|} & \frac{1}{2}nZ'_+ \\ \frac{-\alpha}{2}\eta Z'_- & (\varepsilon-\alpha)\frac{i}{U(\boldsymbol{\kappa})}W^{|m-n|} \end{bmatrix} , \tag{45}$$

$$Z'_{\pm}(\kappa)=\frac{i}{U(\kappa)}\{[W(\kappa)]^{|m-n|}+[W(\kappa)]^{|m-n\pm1|}\}\ , \tag{46}$$

$$U(\kappa)=\begin{cases} i\ \mathrm{sgn}(T)[T^2(\kappa)-1]^{1/2}, & T^2(\kappa)>1 \\ -\mathrm{sgn}\left[\varepsilon-\dfrac{\alpha-1}{2}\right]\sqrt{1-(\kappa)}, & T^2(\kappa)<1 \end{cases} \tag{47}$$

$$T(\kappa)=1+(\varepsilon+1)(\varepsilon-\alpha)\Big/\frac{\alpha}{2}\eta^2(\kappa)\ , \tag{48}$$

$$W(\kappa)=-T(\kappa)-iU(\kappa)\ . \tag{49}$$

From Eqs. (45)–(49), we can easily write down $g(\kappa,E;0,0)$ and $g(\kappa,E;0,-1)$ which are then substituted in (42) to find the SSW spectrum for the free surface with b-sublattice ions. After some algebra, we find

$$\det\begin{vmatrix} 1 & -4J\langle S^z\rangle_a[g_{ab}(0,0)-\eta(\kappa)g_{aa}(0,-1)] \\ 0 & 1-4J\langle S^z\rangle_a[g_{bb}(0,0)-\eta(\kappa)g_{ba}(0,-1)] \end{vmatrix}$$
$$=\frac{4i}{U}\frac{\varepsilon-\alpha}{\alpha^2\eta^4}\left[\varepsilon^2+\left[\frac{1}{2}-\alpha+\frac{\alpha}{2}\eta^2\right]\varepsilon+\frac{\alpha}{2}(\eta^2-1)\right]\left[-iU-T+2\frac{\varepsilon-\alpha}{\alpha\eta^2}+1\right]^{-1}=0\ . \tag{50}$$

Hence the SSW spectrum is determined by the quadratic equation

$$\varepsilon^2+\left[\frac{1}{2}-\alpha+\frac{\alpha}{2}\eta^2\right]\varepsilon+\frac{\alpha}{2}(\eta^2-1)=0\ . \tag{51}$$

The two roots, however, must be rechecked to make sure that the denominator of (50) does not vanish. It turns out that the only solution satisfying all physical conditions is

$$\varepsilon_{b-}(\kappa)=-\frac{1}{2}\left[\frac{1}{2}-\alpha+\frac{\alpha}{2}\eta^2\right]-\frac{1}{2}\left[\left[\frac{1}{2}-\alpha+\frac{\alpha}{2}\eta^2\right]^2+2\alpha(1-\eta^2)\right]^{1/2}\ . \tag{52}$$

As has been pointed out previously, the spin waves are actually the negative energy hole state. Thus the SSW spectrum associated with the free surface of b-sublattice ions is given by

$$\varepsilon^b_{\mathrm{SSW}}(\kappa)=-\varepsilon_{b-}(\kappa)\ . \tag{53}$$

When $\kappa=0$, or $\eta=1$, $\varepsilon^b_{\mathrm{SSW}}(0)=\frac{1}{2}(1-\alpha)$. Hence, this is optical branch for ferrimagnets for which $\alpha<1$ while it represents acoustic branch for antiferromagnets for which $\alpha=1$.

We now turn our attention to the other half space, namely, $m\le-1$, and $n\le-1$. The semi-infinite system in this case has a free surface of a-sublattice ions. Setting $m=-1$ in (39) and following the same procedure as before, we find the Green's function matrix

$$\underline{G}(\kappa,E;m,n)=\underline{g}(\kappa,E;m,n)+[\underline{g}(\kappa,E;m,-1)\underline{V}_{ba}+\underline{g}(\kappa,E;m,0)\underline{V}_{2f}]$$
$$\times[\underline{1}-\underline{g}(\kappa,E;-1,-1)\underline{V}_{ba}-\underline{g}(\kappa,E;-1,0)\underline{V}_{2f}]^{-1}\underline{g}(\kappa,E;-1,n)\ . \tag{54}$$

The SSW spectrum is obtained by solving the determinant equation

$$\det\begin{vmatrix} 1+4\alpha J\langle S^z\rangle_a[g_{aa}(-1,-1)-\eta(\kappa)g_{ab}(-1,0) & 0 \\ 4\alpha J\langle S^z\rangle_a[g_{ba}(-1,-1)-\eta(\kappa)g_{bb}(-1,0) & 1 \end{vmatrix}$$
$$=-\frac{4i}{U}\frac{\varepsilon+1}{\alpha\eta^4}\left[\varepsilon^2+\left[1-\frac{\alpha}{2}-\frac{1}{2}\eta^2\right]\varepsilon+\frac{\alpha}{2}(\eta^2-1)\right]\left[-iU-T-\frac{2(\varepsilon+1)}{\eta^2}+1\right]^{-1}=0\ . \tag{55}$$

Thus the solution of the quadratic equation

$$\varepsilon^2=\left[1-\frac{\alpha}{2}-\frac{1}{2}\eta^2\right]\varepsilon+\frac{\alpha}{2}(\eta^2-1)=0 \tag{56}$$

that does not yield vanishing denominator represents the true SSW spectrum. Again, only one of the two solutions satisfies these conditions and it is

$$\varepsilon_{a+}(\kappa)=-\frac{1}{2}\left[1-\frac{\alpha}{2}-\frac{1}{2}\eta^2\right]+\frac{1}{2}\left[\left[1-\frac{\alpha}{2}-\frac{1}{2}\eta^2\right]^2+2\alpha(1-\eta^2)\right]^{1/2}\ . \tag{57}$$

Thus the semi-infinite system with free surface belonging to a sublattice has only one branch of SSW spectrum

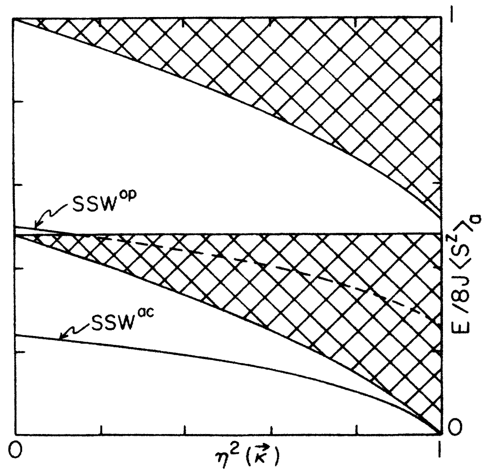

FIG. 5. Optical (op) and acoustic (ac) branches of the SSW spectrum of CsCl structure ferrimagnet, $S_a=1$, $S_b=0.5$, $\alpha=0.481$, and $\langle S^z\rangle_a=0.957$. The corresponding bulk spectrum (shaded area) is shown for comparison.

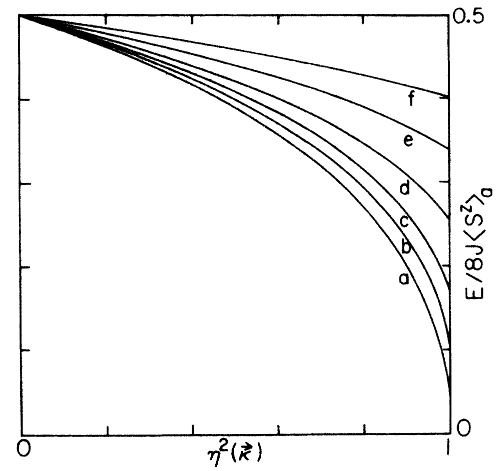

FIG. 7. SSW spectra corresponding to different α values for the surface layer belonging to b sublattice. a: $S_a=S_b$, $\alpha=1$; b: $S_a=2.5$, $S_b=2$, $\alpha=0.796$; c: $S_a=1.5$, $S_b=1$, $\alpha=0.655$; d: $S_a=2$, $S_b=1$, $\alpha=0.489$; e: $S_a=1.5$, $S_b=0.5$, $\alpha=0.32$; f: $S_a=2.5$, $S_b=0.5$, $\alpha=0.194$.

$$\varepsilon^a_{\rm SSW}(\boldsymbol{\kappa})=\varepsilon_{a+}(\boldsymbol{\kappa}) \ . \quad (58)$$

When $\kappa=0$ or $\eta=1$, $\varepsilon^a_{\rm SSW}(\boldsymbol{\kappa})=0$ for any α. Thus it represents acoustic branch of the SSW spectrum.

It is noted that for $\alpha=1$, $\varepsilon^a_{\rm SSW}(\boldsymbol{\kappa})=\varepsilon^b_{\rm SSW}(\boldsymbol{\kappa})$ as expected because the two sublattices are equivalent in antiferromagnets. When this is the case, both (53) and (58) give the identical results as that of Ref. 4 in which the SSW spectrum of a bcc antiferromagnet with a free surface is calculated.

The results of our calculation for different cases are plotted in Figs. 5–8. The shaded area indicates the bulk spectrum continuum. We observe from Fig. 5 that the optical branch of the SSW associated with the (001) free surface of CsCl structure crosses into bulk continuum and forms the resonance state. Such resonant state occurs only when the surface layer belongs to the b sublattice. The SSW spectra corresponding to different α for surface layers belonging to b sublattice and a sublattice are shown in Figs. 7 and 8, respectively. It is seen that the properties of SSW, in the case of CsCl structure, are completely different for surface layers from different sublattices. One has only optical branch and the other can only have acoustic branch.

Although we have restricted our discussions to the (001) free surface of different crystal structures, it is important to point out that the NaCl (111) free surface can be treated in completely the same fashion as the CsCl (001) free surface. In other words, the free surface of semi-infinite crystals with alternative ion layers, each of which contains only one kind of spin, behaves like the CsCl(001) surface as far as the spin-wave spectrum is concerned.

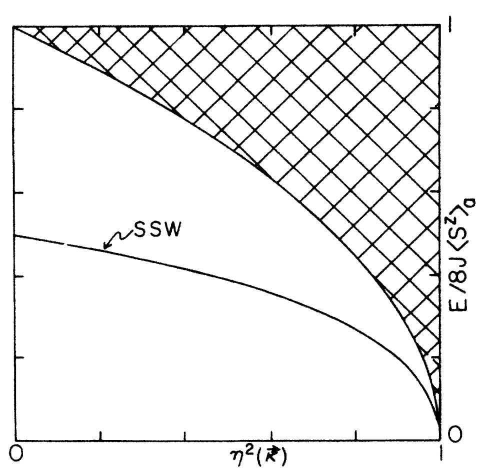

FIG. 6.. SSW spectrum of antiferromagnet with CsCl structure, $S_a=S_b$ and $\alpha=1$. The shaded area shows the corresponding bulk spectrum.

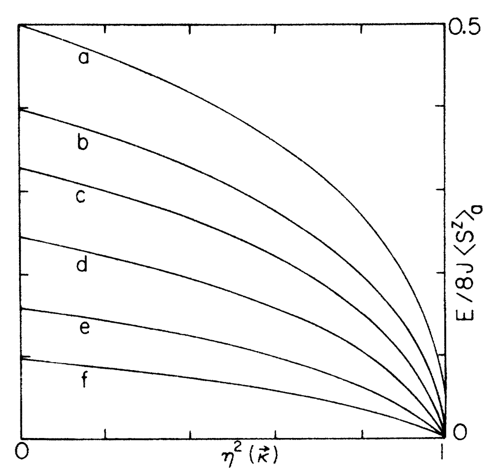

FIG. 8. SSW spectra corresponding to different α values for the surface layer belonging to a sublattice. The curves a–f correspond to the same spins as those of Fig. 7.

V. DISCUSSIONS AND CONCLUSIONS

We have studied the surface spin waves of two-sublattice ferrimagnets by means of the method of retarded-Green's-function equation of motion. Heisenberg model Hamiltonian with nearest-neighbor exchange interaction has been assumed in our discussions. Retarded-Green's-function solutions are obtained for NaCl structure and for CsCl structure with (001) free surface of either a ions or b ions. From these solutions, it is possible to find the SSW density of states, the mean-spin value and its relation to the distance from the surface. It should not be difficult to extend the method to treat the interface problem. Work along these directions is in progress and will be reported in the future.

We have found that for NaCl structure, the SSW spectrum has both optical and acoustic branches, while for CsCl structure the situation is entirely different. When the (001) surface layer belongs to a sublattice, the spectrum has no optical branch and it does not have acoustic branch when the surface belongs to b sublattice. These findings should easily be verified experimentally by choosing different (001) surfaces of ferrimagnets with CsCl structure.

We have also found that the optical branch of SSW spectrum crosses into the acoustic bulk continuum and form the resonance state for CsCl ferrimagnet with b-sublattice surface. The occurrence of such a resonant state is peculiar to this particular type of semi-infinite ferrimagnet. Discussions about such a resonant state can also be found in Refs. 14 and 15.

Finally we note that the above mentioned properties are both characteristic to the CsCl (001) or NaCl (111) surface. Since this may be considered as a structure of alternative layers of a ions and b ions, it may also be regarded as the simplest magnetic superlattice. Therefore, it is not impossible that such peculiar properties may be common to all magnetic superlattices with surface.

APPENDIX

Here we illustrate the method of integration by carrying out the upper left matrix element of $\underline{g}(\boldsymbol{\kappa},E;m,n)$ in (23). We first put the integral in the form

$$g_{aa}(\boldsymbol{\kappa},E;m,n)=\frac{1}{6J\langle S^z\rangle_a}\frac{1}{2\pi}\int_{-\pi}^{\pi}dp\, e^{ip(m-n)}\left[\frac{1+\varepsilon}{\alpha(\alpha-\varepsilon)}\right]^{1/2}\frac{3}{2}\left[\frac{1}{\cos(qd)+T_-(\boldsymbol{\kappa})}-\frac{1}{\cos(qd)+T_+(\boldsymbol{\kappa})}\right], \tag{A1}$$

where we have defined $p=qd$ and

$$T_\pm(\boldsymbol{\kappa})=2\xi(\boldsymbol{\kappa})\pm 3\sqrt{(1+\varepsilon)(\alpha-\varepsilon)/\alpha}\ . \tag{A2}$$

Let $e^{ip}=z$ when $m>n$, and $e^{-ip}=z$ when $m<n$. Then $\cos p=\frac{1}{2}[z+(1/z)]$. The variable z goes around the unit circle in the complex z plane when qd goes from $-\pi$ to π. Therefore, (44) becomes

$$g_{aa}(\boldsymbol{\kappa},E;m,n)=\frac{1}{6J\langle S^z\rangle_a}\frac{3}{2}\left[\frac{1+\varepsilon}{\alpha(\alpha-\varepsilon)}\right]^{1/2}\oint dz\, z^{|m-n|}\left[\frac{2}{z^2+2T_-z+1}-\frac{2}{z^2+2T_+z+1}\right], \tag{A3}$$

which yields directly, by means of residue theorem, the result in (24).

[1] D. L. Mills and A. A. Maradudin, J. Phys. Chem. Solids **28**, 1855 (1967).

[2] R. F. Wallis, A. A. Maradudin, I. P. Ipatova, and A. A. Klockikhin, Solid State Commun. **5**, 89 (1967).

[3] D. L. Mills and W. M. Saslow, Phys. Rev. **171**, 488 (1968).

[4] R. E. DeWames and T. Wolfram, Phys. Rev. **185**, 720 (1969); **185**, 752 (1969); **185**, 762 (1969).

[5] I. Harada and O. Nagai, J. Phys. Soc. Jpn. **42**, 738 (1977); Phys. Rev. B **19**, 3622 (1979).

[6] Diep-The-Hung, J. C. S. Levy, and O. Nagai, Phys. Status Solidi B **93**, 351 (1979).

[7] S. Slazer and N. Majlis, Phys. Rev. B **26**, 404 (1982); **27**, 544 (1983).

[8] A. Yaniv, Phys. Rev. B **28**, 402 (1983).

[9] Bu Xing Xu, M. Mostoller, and A. K. Rajafopal, Phys. Rev. B **31**, 7413 (1985).

[10] L. Dobrzynski, B. Djafari-Rouhani, and H. Puszkarski, Phys. Rev. B **33**, 3251 (1986).

[11] D. L. Lin and H. Zheng, Phys. Rev. B **37**, 5394 (1988).

[12] Fu-Cho Pu, Dol. Adad. Nauk. USSR **130**, 1244 (1960) [Sov. Phys.-Doklady **131**, 546 (1960)].

[13] N. N. Bogoliubov, and S. V. Tyablikov, Dokl. Acad. Nauk SSSR **126**, 53 (1959) [Sov. Phys.-Doklady **4**, 589 (1959)].

[14] R. Tahir-Kheli and D. ter Haar, Phys. Rev. **127**, 88 (1962).

[15] H. B. Callen, Phys. Rev. **130**, 890 (1963); **131**, 540 (1963).

[16] D. Kalkstein and P. Soven, Surf. Sci. **26**, 85 (1971).

[17] See, for example, *Handbook of Applied Mathematics*, edited by C. E. Pearson (Van Nostrand Reinhold, New York, 1974).